

LA-UR -81-1556

TITLE: PRETEST AND POSTTEST CALCULATIONS OF SEMISCALE TEST S-07-10D
WITH THE TRAC COMPUTER PROGRAM

AUTHOR(S): K. H. Duerre, G. E. Cort, and T. D. Knight

MASTER

SUBMITTED TO: American Nuclear Society Specialists Meeting
on Small Break Loss of Coolant Accident Analysis
in LWR's, Monterey, CA, August 25-27, 1981



By acceptance of this article, the publisher recognizes that the U.S. Government retains a nonexclusive, royalty free license to publish or reproduce the published form of this contribution, or to allow others to do so, for U.S. Government purposes.

The Los Alamos Scientific Laboratory requests that the publisher identify this article as work performed under the auspices of the U.S. Department of Energy.

REPRODUCTION OF THIS DOCUMENT IS UNLIMITED

University of California



LOS ALAMOS SCIENTIFIC LABORATORY

Post Office Box 1663 Los Alamos, New Mexico 87545

An Affirmative Action/Equal Opportunity Employer

PRETEST AND POSTTEST CALCULATIONS OF SEMISCALE TEST S-07-10D
WITH THE TRAC COMPUTER PROGRAM*

K. H. Duerre
Technical Engineering Support Group
Los Alamos National Laboratory
Los Alamos, NM 87545
Telephone: (505) 667-7376

G. E. Cort
Technical Engineering Support Group
Los Alamos National Laboratory
Los Alamos, NM 87545
Telephone: (505) 667-5726

T. D. Knight
Safety Code Development Group
Los Alamos National Laboratory
Los Alamos, NM 87545
Telephone: (505) 667-3113

ABSTRACT

The Transient Reactor Analysis Code (TRAC) developed at the Los Alamos National Laboratory was used to predict the behavior of the small-break experiment designated Semiscale S-07-10D. This test simulates a 10 per cent communicative cold-leg break with delayed Emergency Core Coolant injection and blowdown of the broken-loop steam generator secondary. Both pretest calculations that incorporated measured initial conditions and posttest calculations that incorporated measured initial conditions and measured transient boundary conditions were completed.

The posttest calculated parameters were generally between those obtained from pretest calculations and those from the test data. The results are strongly dependent on depressurization rate and, hence, on break flow. The calculated results appear to be conservative; that is, higher clad temperatures are calculated that are the result of faster depressurization. The code appears to calculate correctly trends in the data, including the mass distribution of liquid (although slightly clouded by the small make-up flow that was not modeled). We believe that the comparison of calculated and measured results would be improved if a critical flow model had been available for the small break.

*This work was performed under the auspices of the US Nuclear Regulatory Commission.

I. INTRODUCTION

The Semiscale test program is designed to provide coupled thermal-hydraulic effects data from a scaled Pressurized Water Reactor (PWR).¹ The volumetric scaling is approximately 1:3000. The data are used to assess the ability of computer codes to predict the Loss-of-Coolant Accident (LOCA) response of a PWR.

The Transient Reactor Analysis Code (TRAC) computer program is a state-of-the-art, best-estimate code developed at Los Alamos.² Although the code was designed primarily for the analysis of large-break LOCAs, it can be applied directly to a wide variety of analyses, including the Small-Break Experiment (SBE) described here. Comparisons are given in this paper of TRAC predictions vs preliminary data obtained from the Semiscale test designated S-07-10D. This test simulates a 10 per cent communicative cold-leg break with delayed Emergency Core Coolant (ECC) injection and blowdown of the broken-loop steam-generator secondary.

Two sets of calculations were performed.

1. Pretest calculations with TRAC-PIA that incorporated measured initial conditions,* and
2. Posttest calculations with TRAC-PD2 that incorporated measured initial conditions and measured transient boundary conditions.

II. MODEL DESCRIPTION

A. Physical Model

The Semiscale Mod 3 model is shown in Fig. 1. The intact loop was designed to represent three of the four loops normally associated with a PWR.

B. TRAC Pretest Model

This calculative model is shown in Fig. 2 and consists of 26 components identified in Table 1. The components have a total of 222 cells. All components are one dimensional except the vessel, which is three dimensional. The break orifice was represented by a flow area restriction in the side tube of component 25, a tee. The side tubes of components 25 and 27 (the broken loop steam generator steam line) used fully implicit numerics. The remaining components were semi implicit. The accumulator valve, component 11, was initially tripped open on pressure and then changed on restart to a check valve. Built in Semiscale pump curves were used for both pumps.

*The measured initial conditions for the pretest calculations were based on Semiscale S-07-10B rather than S-07-10D. The difference is not significant.

TABLE I
SYSTEM MODEL COMPONENTS

<u>Component Number</u>	<u>Component Type</u>	<u>Description</u>	<u>Cells</u>
1	TEE	Intact-loop hot leg	4, 3
2	STGEN	Intact-loop steam generator	10, 6
3	PIPE	Intact-loop pump suction	21
4	PUMP	Intact-loop pump	2
5	TEE	Intact-loop cold leg	4, 1
6	PRIZER	Pressurizer	5
7	FILL	Intact-loop steam-generator feedwater	1
8	VALVE	Intact-loop steam-generator steam line	2
9	BREAK	Intact-loop steam-generator back pressure	1
10	TEE	Intact-loop ECC injection line	2, 1
11	VALVE	Intact-loop accumulator valve	2
12	ACCUM	Intact-loop accumulator	4
13	FILL	Intact-loop High Pressure Injection System and Low Pressure Injection System	1
21	PIPE	Broken-loop hot leg	3
22	STGEN	Broken-loop steam generator	12, 6
23	PIPE	Broken-loop pump suction	19
24	PUMP	Broken-loop pump	2
25	TEE	Broken-loop cold leg	4, 1
26	FILL	Broken-loop steam generator feedwater	1
27 ^a	PIPE	Broken-loop steam generator steam line	16
28	BREAK	Broken-loop steam generator back pressure	1
40	BREAK	Small break back pressure (containment)	1
51	PIPE	Upper head bypass piping	3
52	PIPE	Guide tube simulator	3
53	PIPE	Core support tube simulator	3
50	VESSEL	Inlet annulus, downcomer, and vessel (lower plenum, core, upper plenum, and upper head) / radial rings, 1 theta segments, 19 axial levels.	26

^aOmitted in posttest run.

Figure 3 shows the vessel nodalization. The following Semiscale components are represented by the vessel: the inlet annulus, the downcomer, the upper and lower plenums, the core, and the upper head. The vessel was modeled with two radial rings, two theta segments, and 19 vertical levels. The core was located in ring 1, levels 4 through 12. The high- and low-powered rods in Semiscale were modeled as hot rods in each of the two core channels with correct peaking factors specified. Reflood fine-mesh noding (7.62 cm interval) in the core was tripped at the beginning of accumulator injection. Re-entrant pipe components 51, 52, and 53 represented the inlet annulus-to-upper head bypass, the core support tube simulators, and the guide tube simulator, respectively.

C. TRAC Posttest Model

The posttest input was basically the same as that for the pretest model. The broken-loop steam-generator steam line (component 27) was removed from the pretest model, and measured pressure was specified at break component 28 to better simulate the blowdown transient. Several minor changes were made to the pretest model, the most significant being the addition of friction to the core and downcomer. Table II gives a brief summary of these changes.

The model was based primarily on Semiscale Mod-3 drawings,³ with additional information obtained from Semiscale documents.^{1,4-8}

III. STEADY-STATE CALCULATIONS

The TRAC generalized steady-state option was used for both calculation sets. A stagnant, isothermal condition was the starting point for the steady state calculation, followed by real-time runs of 110 s for the pretest run and 180 s for the posttest run. Table III gives the measured initial conditions for the transient and corresponding conditions specified or calculated by TRAC. The specified conditions for the pretest run were obtained from Semiscale test S-07-108, (Ref. 4) which differed slightly from the initial conditions of Semiscale test S-07-100 (Refs. 5 and 9-10) shown in Table III.

The steam-generator steam-side boundary conditions were not accurately known, so this component was isolated and trial runs were made to achieve the correct primary exit fluid temperature. Specifying the known dome pressure and a change of tube material for the posttest case caused the different initial conditions for the steam generators shown in Table III.

IV. TRANSIENT RESULTS

The test was initiated with the opening of the small break and proceeded until approximately 750 s. Several trips were initiated 1 s after pressurizer pressure dropped to 12.41 MPa. Core power decay began, the pumps began coast down, and the steam generator feedwater valves began to close. The intact loop steam generator steam valve closed after 20 s. The pressure suppression system reduced break pressure during the interval 50 to 150 s. The Manual Emergency

TABLE II

CHANGES MADE BETWEEN THE PRETEST AND POSTTEST TRAC SEMISCALE MODELS

1. The pretest model was run with TRAC-P1A. The posttest model used TRAC-PD2.^a
2. The axial nodalization in the heater rods was modified to conform to differing input requirements between the two TRAC versions and to match the locations of computed temperatures with the thermocouple locations.
3. Additive loss coefficients simulating friction were added to the core and downcomer. These were based on pressure drop measurements from the Semiscale baseline test series.¹
4. Small changes were made in the vessel radius to match closely the as-built volume.
5. The additive loss coefficient in the pipe leading to the break was increased by one-third to reduce break flow.
6. The material properties for the steam generator tubes were changed to correspond with Inconel 600 alloy rather than Inconel 718.
7. Changes to the uncertain flow resistance in the broken-loop steam line were eventually abandoned after preliminary calculations. Instead, the steam dome pressure was specified to be equal to the measured value for the transient.

^aTRAC PD2 contains major improvements in the areas of reflood heat transfer, solution strategy, numerics, constitutive relations, and numerical mass conservation.

TABLE III
SEMISCALE TEST S-07-10D INITIAL CONDITIONS

<u>Parameter</u>	<u>Test</u>	<u>Calculated</u>	
		<u>Pretest</u>	<u>Posttest</u>
Nominal System Pressure (MPa)	15.73	15.701	15.73
Intact-Loop Fluid Temperatures (K)			
Hot leg	593	591.6	593.6
Cold leg	556	555.7	556.9
Broken-Loop Fluid Temperatures (K)			
Hot leg	591	591.6	593.7
Cold leg	558	556.2	562.8
Flow Rate (kg/s)			
Intact loop	7.45	7.541	7.474
Broken loop	2.27	2.315	2.296
Upper head bypass (%)	4.2	4.2	4.28
Total-Core Power (MW)	1.925	1.94	1.927
Radial peaking factor (high-power rod above low-power rod)	1.52	1.6244 ^a	1.52
Pump Speeds (rad/s)			
Intact loop	240	242	242
Broken loop	1620 ^b	1372	1372
Pressurizer Liquid Mass (kg)	10.4	9.49	10.33
Intact-Loop Accumulator			
Pressure (MPa)	3.102 ^b	2.74	2.74
Actuation pressure (MPa)	1.6	1.45	1.6
Liquid volume (m ³)	0.045	0.045	0.045
Gas volume (m ³)	0.025	0.025	0.025
Temperature (K)	300	300	300
Steam Generator Secondaries			
Intact Loop Steam Dome			
Pressure (MPa)	6.64 ^b	5.367	5.573
Temperature (K)	544	541.5	544
Broken-Loop Steam Dome			
Pressure (MPa)	6.26	5.483	6.45
Temperature (K)	551	543	552

^aTest S-07-10B had this higher peaking factor.

^bThis higher value was not reported until calculations were completed; however, the effect on measured results was judged to be insignificant (Ref. 9).

Core Cooling System (ECCS) injection was delayed until elevated cladding temperatures occurred in the core. The Low Pressure Injection System (LPIS) injection was initiated at the same time, but significant LPIS flow did not begin until approximately 100 s after the ECCS injection and after the core had quenched.

Table IV lists measured and calculated times for occurrence of significant events during the transient. In Figs. 4-18, the solid line is the posttest calculation; the test results and the pretest calculations are dotted lines with circle and triangle symbols as indicated.

Figure 4 shows the upper plenum pressure. The pressure at saturation is overpredicted and the changes in slope of the calculated pressure transient after saturation (30 to 400 s) are not matched by the data. The overprediction is related to the higher than measured hot-leg temperatures (Table III), but the changes in slope cannot be explained. All of the five calculative methods used to simulate this test showed this same general tendency in slope of the upper plenum pressure, and none matched the slope of the measurement in this time interval.⁹ The pressure increase about halfway through the transient corresponds to the beginning of core quench. Note that the posttest results are between the pretest and the test results. A one-third greater loss coefficient in the side tube of the tee adjacent to the break and the inclusion of friction in the core and downcomer contributed to the 40 s delay in the posttest pressure rise compared to the pretest case. The ECCS injection was triggered on pressure, 1.45 MPa for pretest and 1.6 MPa for posttest. The delay would have been even greater if the trip had occurred at 1.6 MPa in the pretest calculation.

Figure 5 shows the accumulator volume flow. In the pretest calculation, accumulator flow was initiated by a 1.45 MPa system pressure trip at 368 s compared to the posttest calculation, which was initiated by a trip at 1.6 MPa at 407 s. As system pressure increased with core quenching, the accumulator flow ceased, with a second period of flow around 500 s. An offset of approximately 100 s for the test data corresponds to the pressure delay of Fig. 4.

Figures 6 through 9 show conditions around the break. The increase in break flow (Fig. 6) for the test at 50 s was postulated to be caused by flashing in the intact-loop steam-generator primary, forcing flow through the broken-loop hot leg.⁵ This increase in flow following accumulator injection is slight for posttest calculations compared to the test and pretest calculation. The posttest break flow is underpredicted, consistent with the overprediction of system pressure. The density on the pump side in the tee adjacent to the break (Fig. 7) was consistently lower for the calculated cases until accumulator injection occurred, when the pretest calculation curve rose to intersect the test density, and then remained higher after 450 s for the remainder of the test. The steady-state make-up flow in the broken-loop cold leg was inadvertently left on during the first 150 s of the transient test. This resulted in 0.0373 kg/s of ambient water being injected upstream of the break. Posttest calculations with RELAP4 by the Idaho National Engineering Laboratory showed an insignificant effect on the primary system pressure.⁹ The make-up flow was not included in the TRAC model; if included, it could

TABLE IV
SEQUENCE OF EVENTS FOR SEMISCALE TEST S-07-10D

<u>Event</u>	<u>Test</u>	<u>Time (s)</u>	
		<u>Pretest</u>	<u>Posttest</u>
Initiate transient by opening break	0.0	0.0	0.0
12.41 MPa pressurizer pressure trip to initiate core power decay, pump coast-down and steam generator isolation	6.8	6.3	6.7
Broken-loop steam-generator feedwater at zero flow	10	9.3	9.5
Intact-loop steam-generator steam line valve closes	21	20	23
Pressurizer empties	20	20	20
Pumps stop	79	75.3	77
Core dryout occurs and cladding temperature starts to increase	268	172	210
Core voided ^a	435	330	412
HPIS and accumulator injection begin	458	368	407
Cladding temperatures turn over	468	377	415
Core quenched	525	447	500
Significant LPIS injection begins	560	468	507

^aVoiding is based on the calculated liquid volume fraction and the measured differential pressures, densities, and velocities.⁹ For the posttest analysis, the core is not completely voided, but the minimum liquid volume fraction of 0.13 is reached before ECC injection (Fig. 14).

have improved the agreement. The make-up flow was not left on during the transient for the S-07-10B test, and the measured density in the broken-loop cold leg was lower than was measured in the S-07-10D test. This apparent inconsistency indicates that the density was affected by other (unknown) parameters more strongly than by the make-up flow. The density on the vessel side of the break (Fig. 8) shows a somewhat opposite effect, with a higher density consistently calculated after about 50 s until 200 s where the curves converge. Figure 9 shows a calculated flow reversal in the broken-loop primary piping between the vessel and the break at about 40 s in the posttest calculation and at 70 s in the pretest calculation, until about 180 s when both flows became approximately zero.

Conditions at the broken-loop steam generator are shown in Figs. 10 and 11. The steam dome pressure was specified for the steady-state and transient posttest calculation, but was calculated for the pretest. The poor match shown in Fig. 10 for the pretest calculation may be caused by lack of information about the steam-line geometry and the unknown quality of steam leaving the secondary. The effect of this is readily seen in Fig. 11 where the posttest calculated primary fluid exit temperatures are close to the test values, but the pretest calculations diverge from them. As the tubes voided, the heat transfer from the primary to the secondary decreased and the secondary side became a heat source by 190 s.

The remaining figures depict vessel behavior. The downcomer liquid volume fraction (Fig. 12) shows the downcomer slowly emptying until the accumulator and High Pressure Injection System (HPIS) flow began, when it filled rapidly. As the core began to quench, liquid was forced out of the downcomer by flow oscillations. The differences between pretest and posttest calculations were caused by (1) friction added to the posttest model and (2) a lower pressure trip for the pretest model. The liquid temperature (Fig. 13) followed the saturation temperature until the downcomer was filled with subcooled water. Heat transfer from the walls and flow from the core subsequently caused a slow warming of the liquid. The second period of accumulator injection around 500 s was followed by a second warming trend.

The core liquid volume fraction and the upper plenum liquid volume fraction (Figs. 14 and 15) show the same slow emptying and rapid refill that typified the downcomer. The start of oscillations in the posttest calculations coincide with the start of significant HPIS injection at 507 s, and the 8-s period calculated by TRAC corresponds to the expected period for manometer oscillation with the liquid length extending from the cold leg inlet in the downcomer to the vessel upper plenum. The oscillations also show up in the core inlet mass flow rate (Fig. 16), with flow reversals occurring as the liquid sloshes back and forth. The core inlet mass flow follows the test data reasonably well except that the measured flow is slightly greater after 100 s. Oscillations in the measured flow are present, but with lower amplitude than calculated.

The posttest high-power-rod cladding temperature at several levels is shown in Fig. 17. Both the low- and high-power rods illustrate the early response and higher temperatures achieved near the midplane where power generation is greatest. Cladding temperatures turned over at 377 s for the pretest

calculation, 415 s for the posttest calculation, and 468 s for the test. The peak cladding temperatures for pretest, test, and posttest were 1249, 1145, and 1195 K, respectively, in the high-power rods. The timing for the peak cladding temperature is highly dependent on the time of ECC injection.

Figure 18 illustrates a "typical" cladding temperature vs time profile for the high-power rod. The core elevation was not precisely the same for pretest, posttest, and test results; however, it can be seen that the posttest results are intermediate in time, indicating a strong dependence on the depressurization rate.

V. CONCLUSIONS

The posttest calculation values were generally between those obtained from pretest calculations and test data. The calculated results appear to be conservative; that is, higher clad temperatures are calculated that are the result of faster depressurization. The results are strongly dependent on depressurization rate and, hence, on break flow. The TRAC-PD2 program appears capable of predicting mass distribution and system behavior reasonably well. We feel, however, that the comparison of calculated and test results would have been closer if a critical flow model had been available for the small break.

REFERENCES

1. D. H. Miyasaki, K. E. Sackett, and D. R. Pack, "Experiment Data Report for Semiscale Mod-3 Lower Plenum Injection Test S-07-9 (Baseline Test Series)," EG&G Idaho, Inc. report NUREG/CR-0815 (TREE-1229) (June 1979).
2. "TRAC-PD2: An Advanced Best-Estimate Computer Program for Pressurized Water Reactor Loss-of-Coolant Accident Analysis," Los Alamos National Laboratory report LA-8709-MS (February 1981).
3. M. L. Patton, "Semiscale Mod-3 Test Program and System Description," EG&G Idaho, Inc. report NUREG/CR-0239, TREE-NUREG-1212 (July 1978).
4. EG&G Idaho, Inc. letter, D. J. Olson to R. E. Tiller, DJO-30-79, "Transmittal of Initial Conditions for Semiscale Mod-3 Test S-07-10B (Small Break Test)," February 22, 1979.
5. EG&G Idaho, Inc. letter, L. P. Leach to R. E. Tiller, LPL-112-80, "Transmittal of Analysis Report for Semiscale Mod-3 Tests S-07-10 and S-07-10D," June 27, 1980.
6. EG&G Idaho, Inc. letter, L. P. Leach to R. E. Tiller, LPL-64-80, "Experimental Operating Specification for Test S-07-10C," May 7, 1980.

7. EG&G Idaho, Inc. letter, L. P. Leach to R. E. Tiller, LPL-28-80, "Preliminary Data Release for Semiscale Mod-3 Test S-07-10B," February 26, 1980.
8. EG&G Idaho, Inc. letter, D. J. Olson to R. E. Tiller, DJO-150-78, "Experimental Operating Specification for Test S-07-10," November 27, 1978.
9. C. A. Dobbe, "Small Break Experiment (Semiscale S-07-10D) Preliminary Comparison Report," EG&G Idaho, Inc. interim report EGG-CAAP-5279 (December 1980).
10. K. E. Sackett and L. Bruce Clegg, "Experiment Data Report for Semiscale Mod-3 Small Break Test S-07-10D (Baseline Test Series)," EG&G Idaho Inc., report NUREG/CR-1641 (EGG-2065) (December 1980).

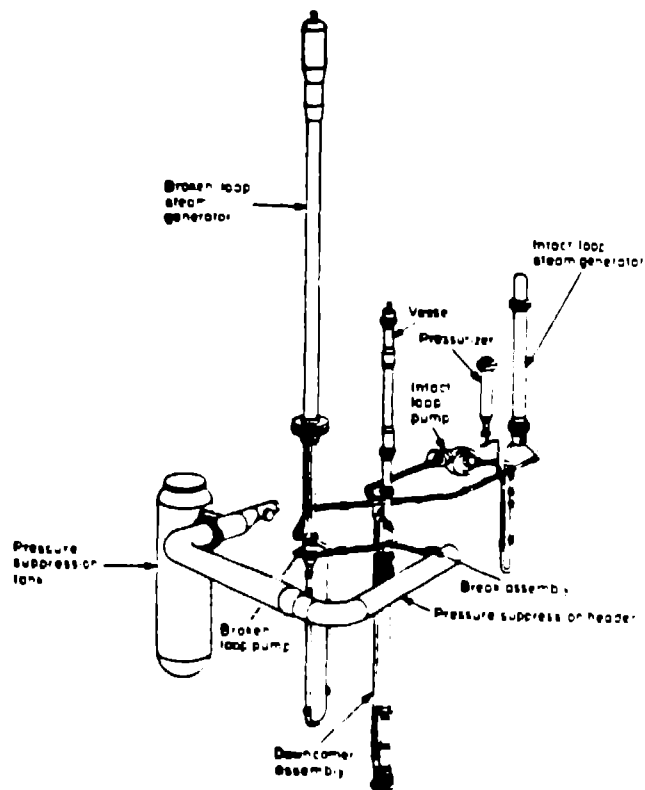


Fig. 1. Semiscale Mod-3 system cold-leg communicative small-break configuration isometric.

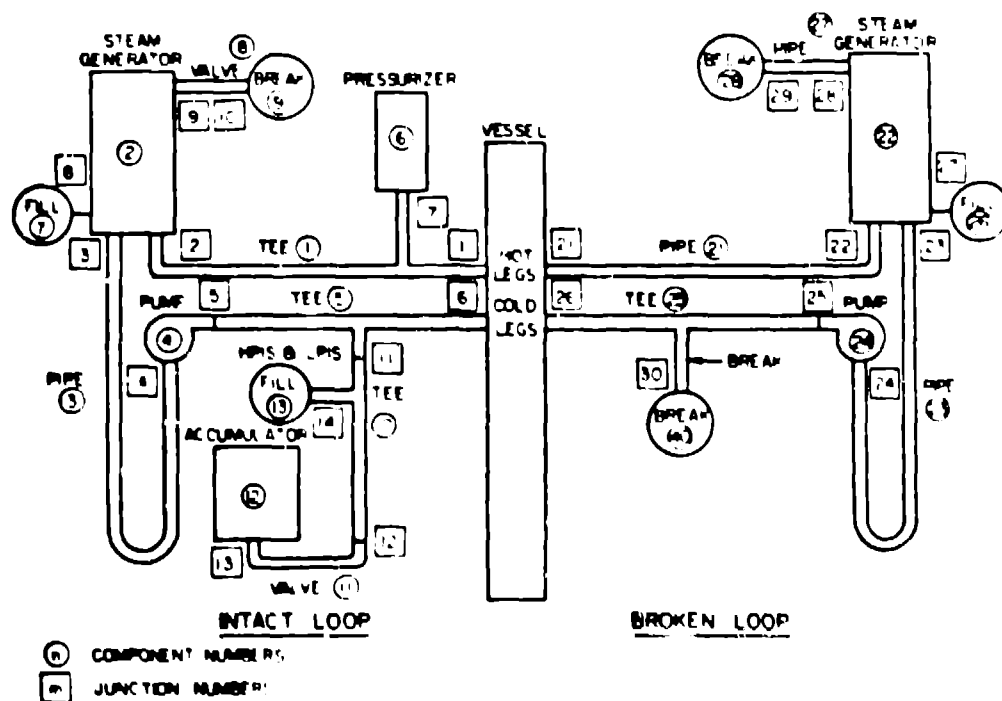


Fig. 2. TRAC pretest model of Semiscale Mod-3 facility. The posttest model eliminated component 27, the broken-loop steam line.

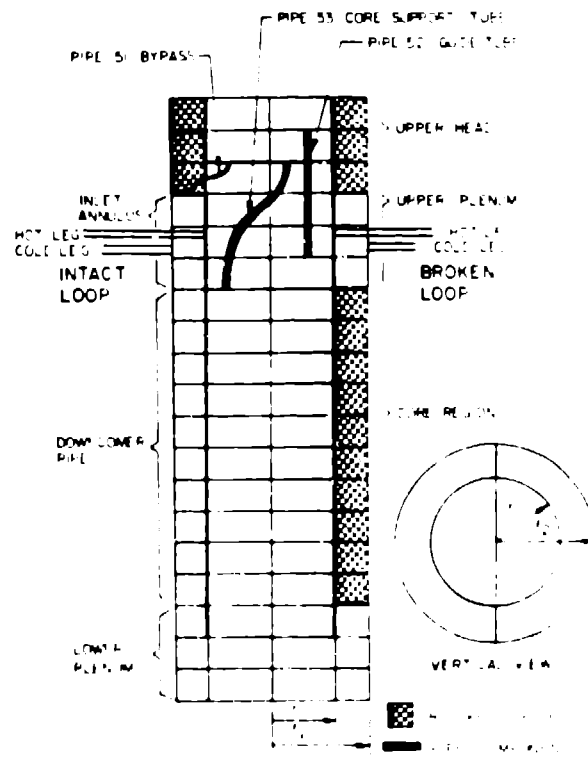


Fig. 3. Vessel nodalization.

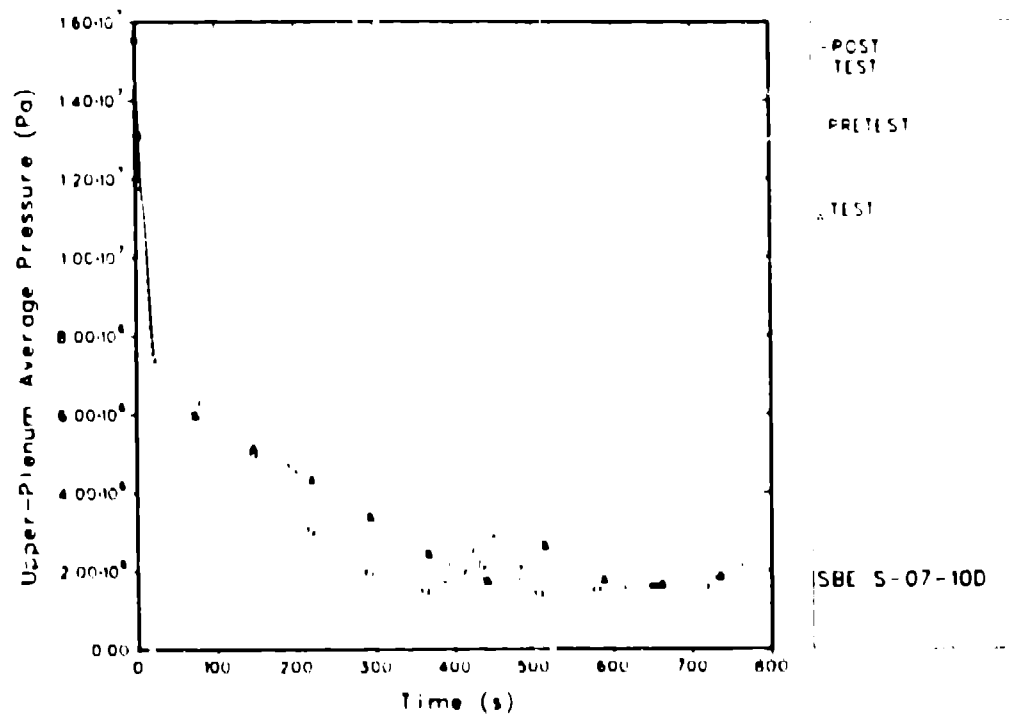


Fig. 4. Upper plenum pressure.

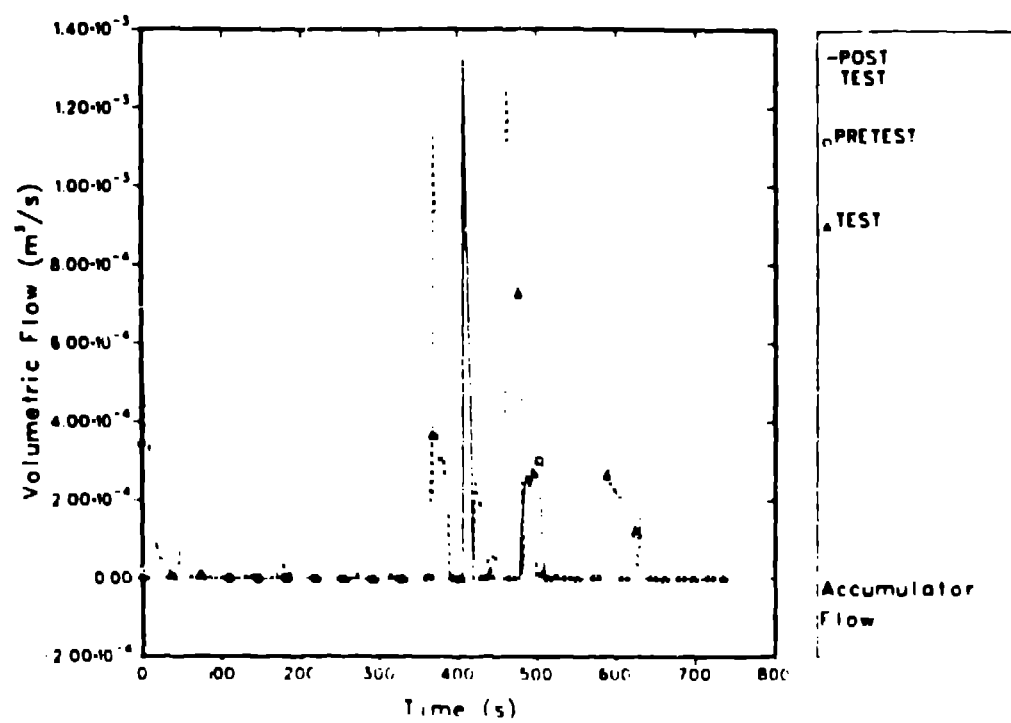


Fig. 5. Accumulator flow.

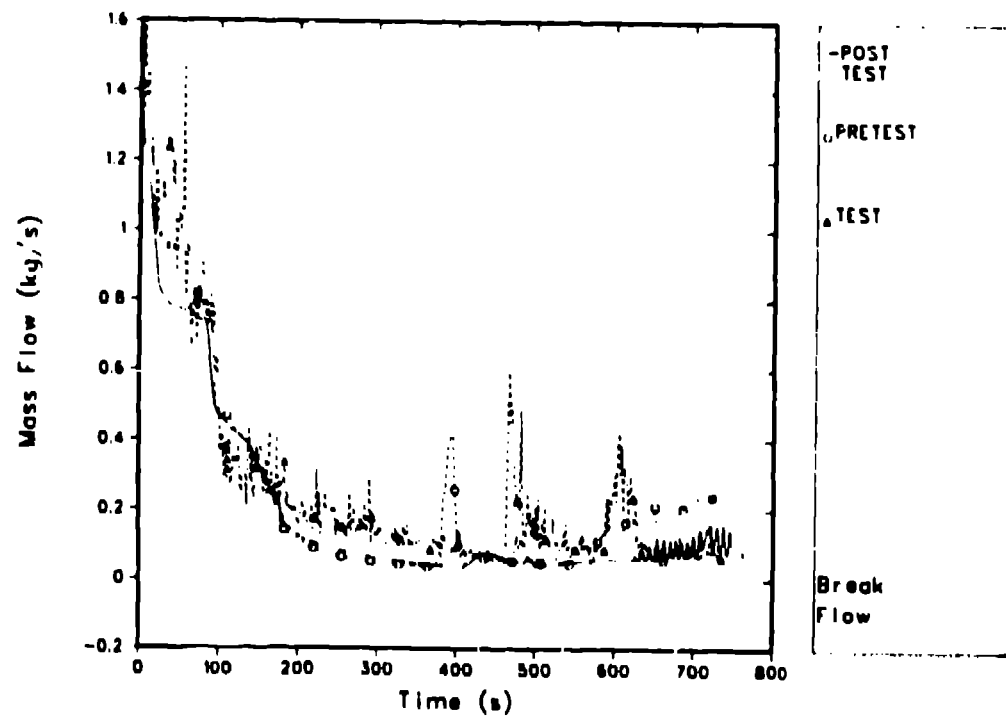


Fig. 6. Mass flow rate at the break.

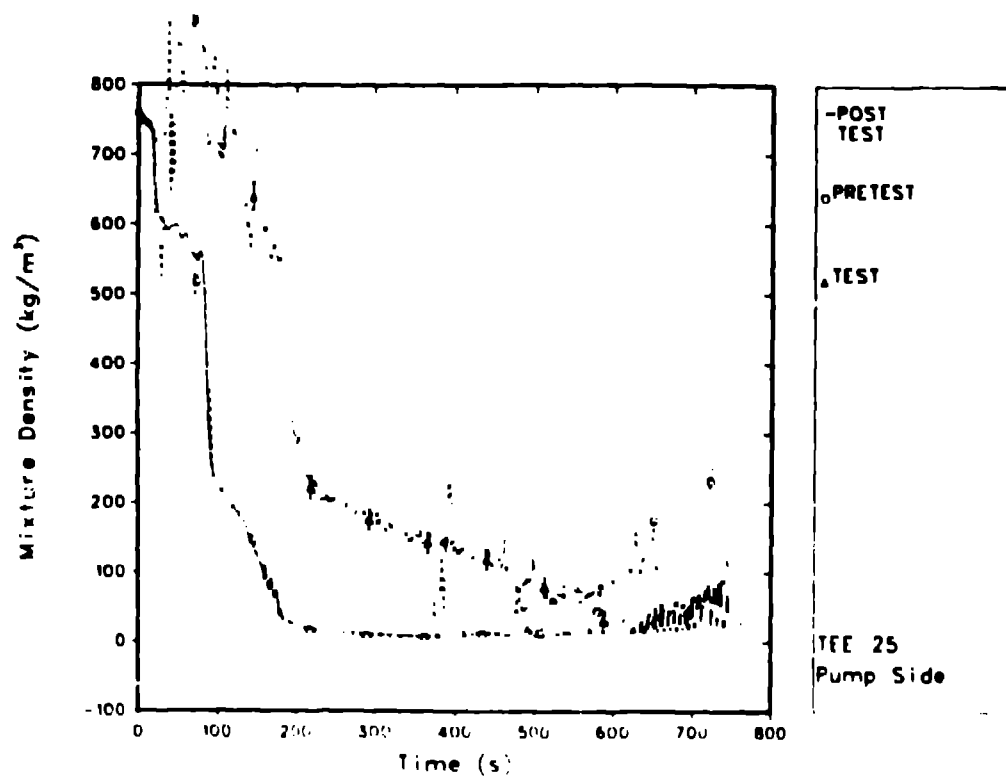


Fig. 7. Mixture density in broken-loop cold leg upstream of the break.

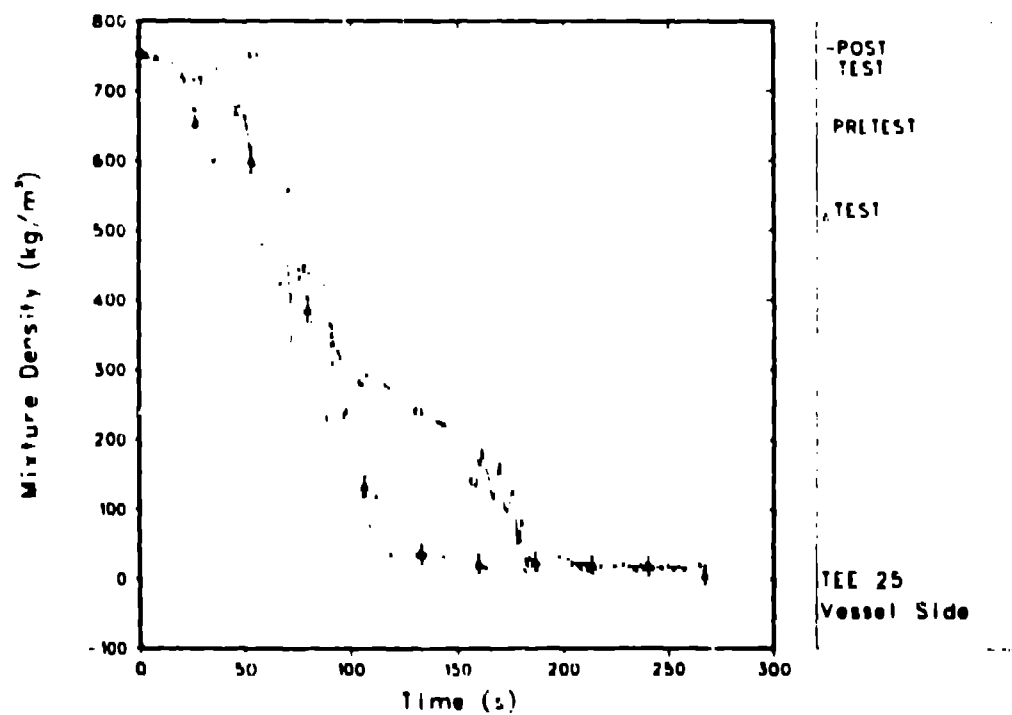


Fig. 8. Mixture density in broken-loop cold leg downstream of the break.

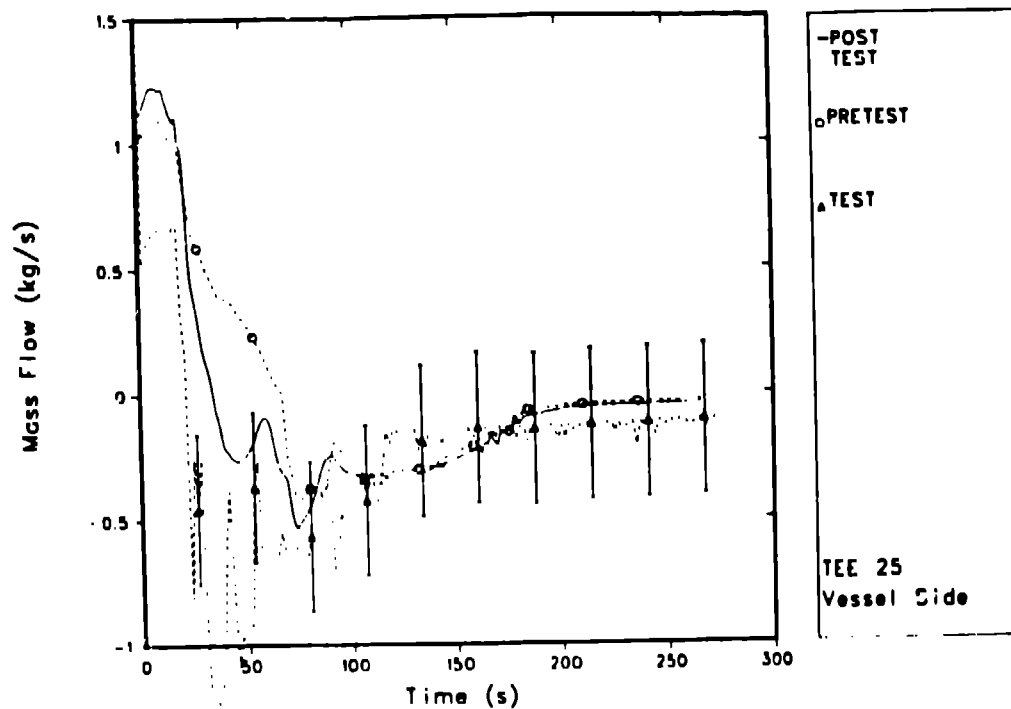


Fig. 9. Mass flow in the broken-loop cold leg downstream of the break.

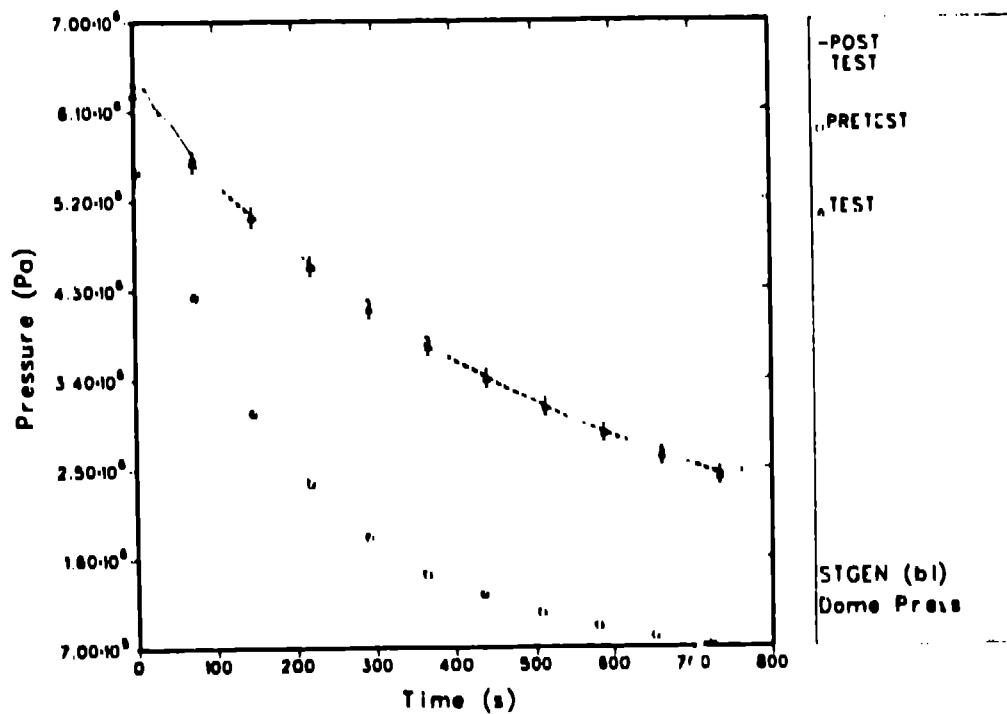


Fig. 10. Broken-loop steam generator steam dome pressure.

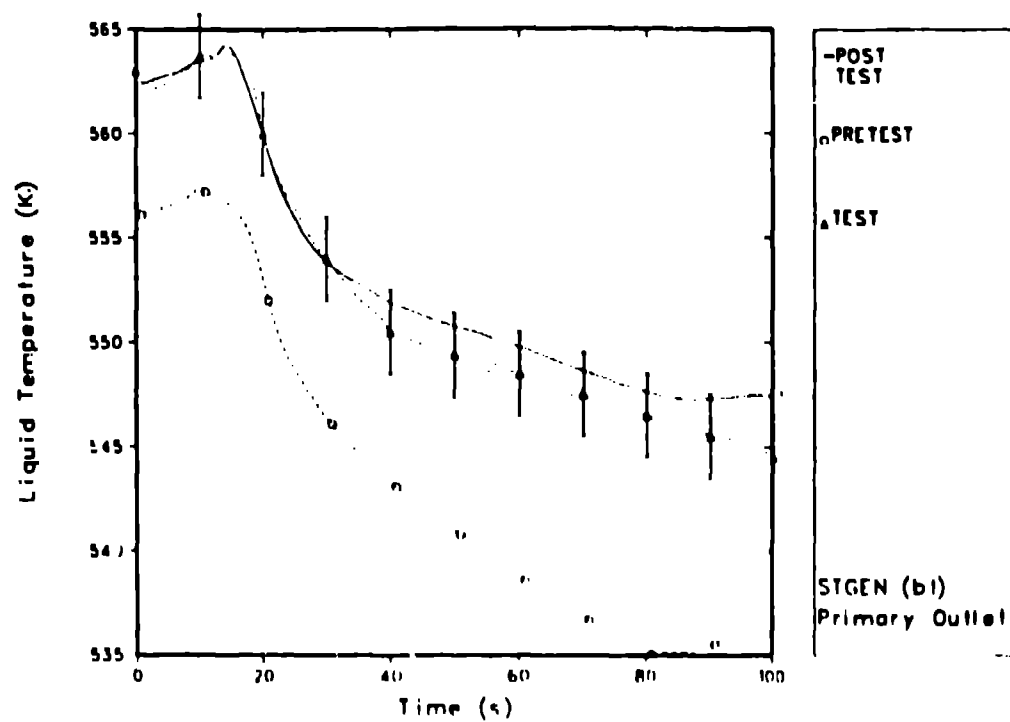


Fig. 11. Broken-loop steam generator liquid temperature.

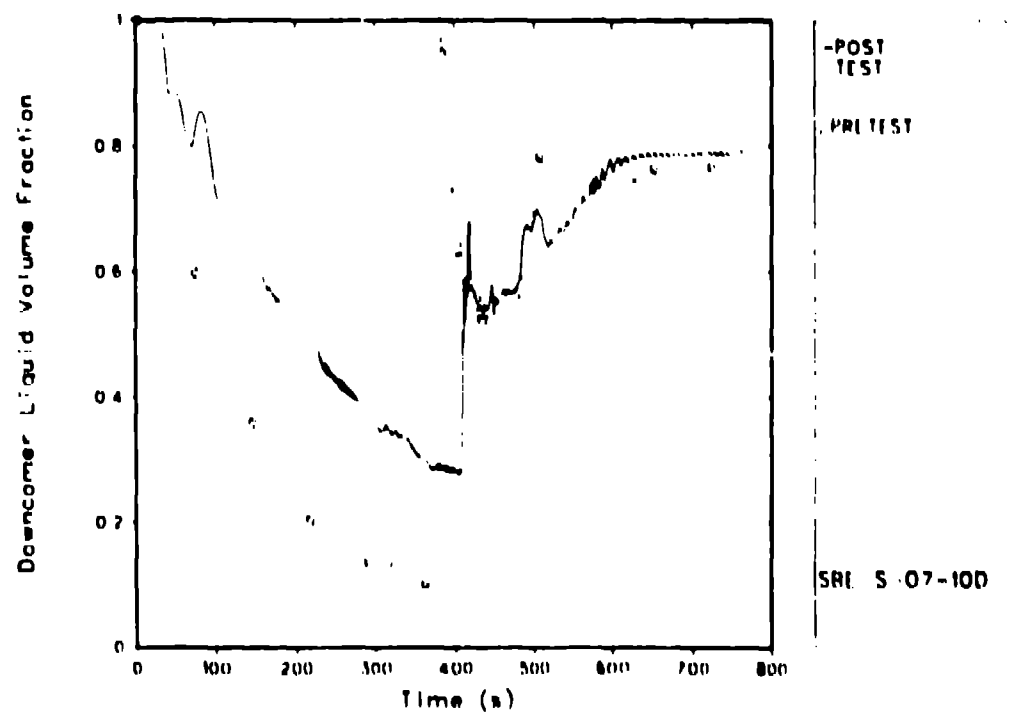


Fig. 12. Downcomer liquid volume fraction.

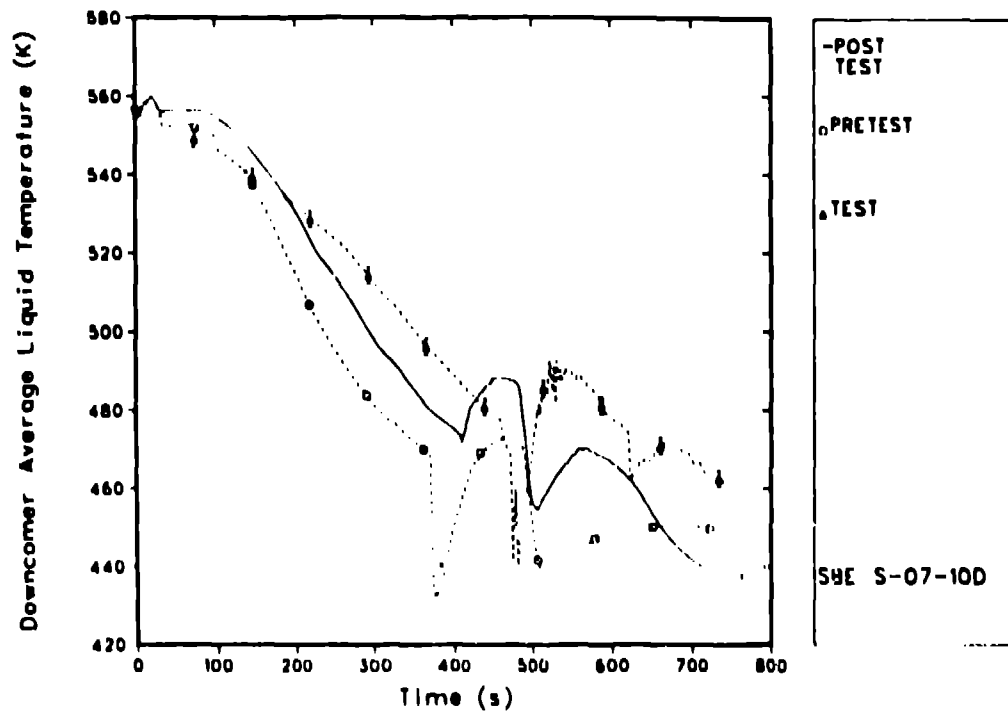


Fig. 13. Downcomer average liquid temperature.

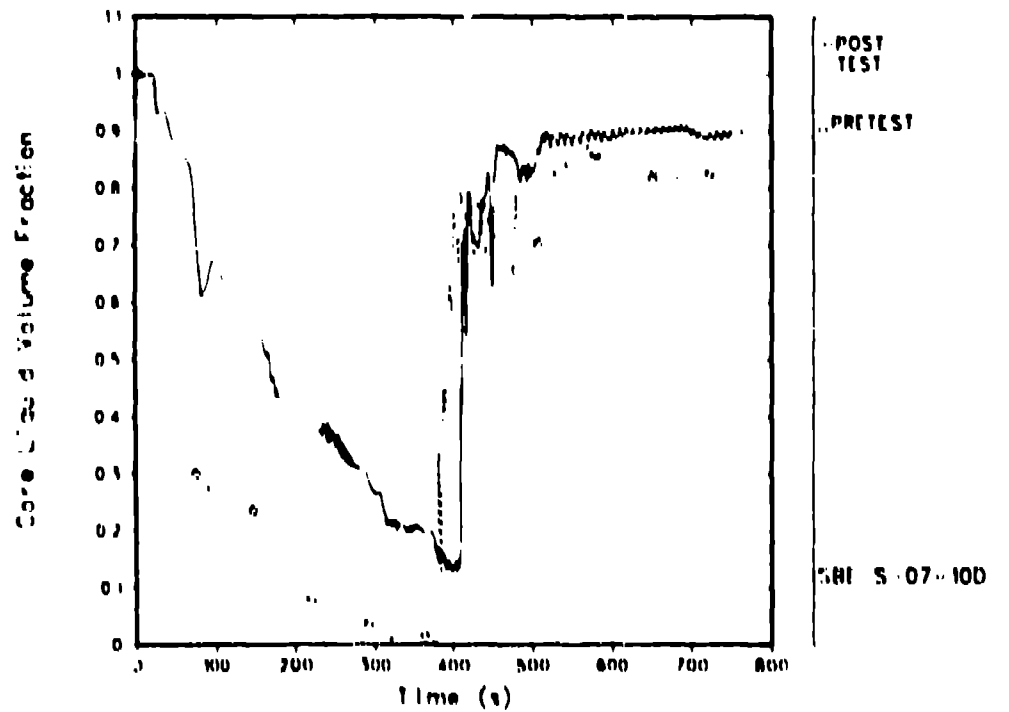


Fig. 14. Core liquid volume fraction.

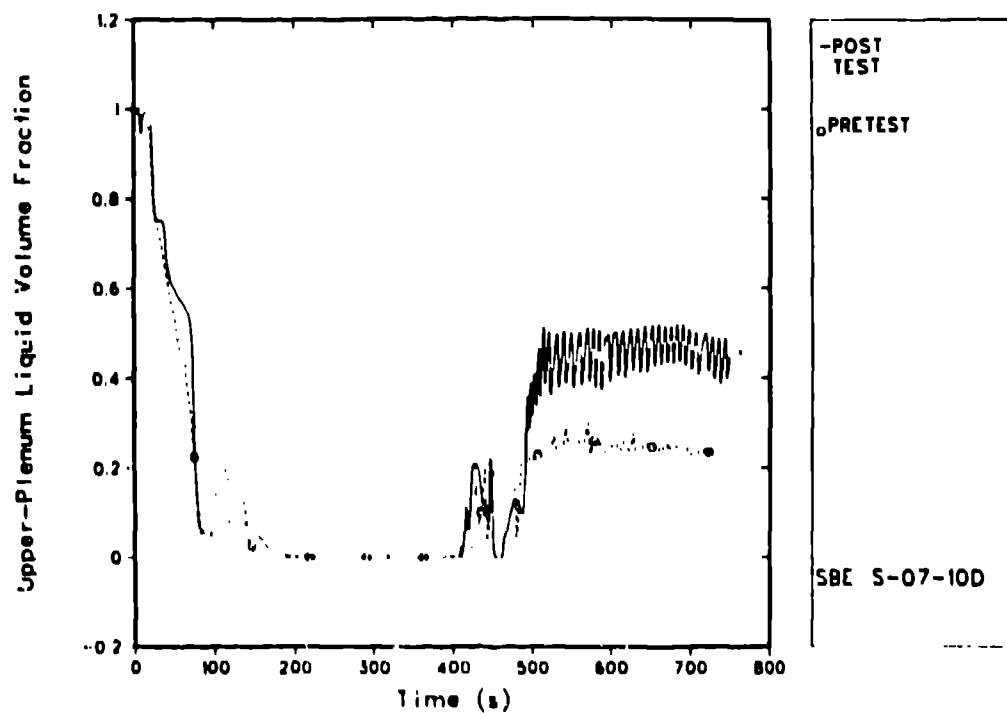


Fig. 15. Upper-plenum liquid volume fraction.

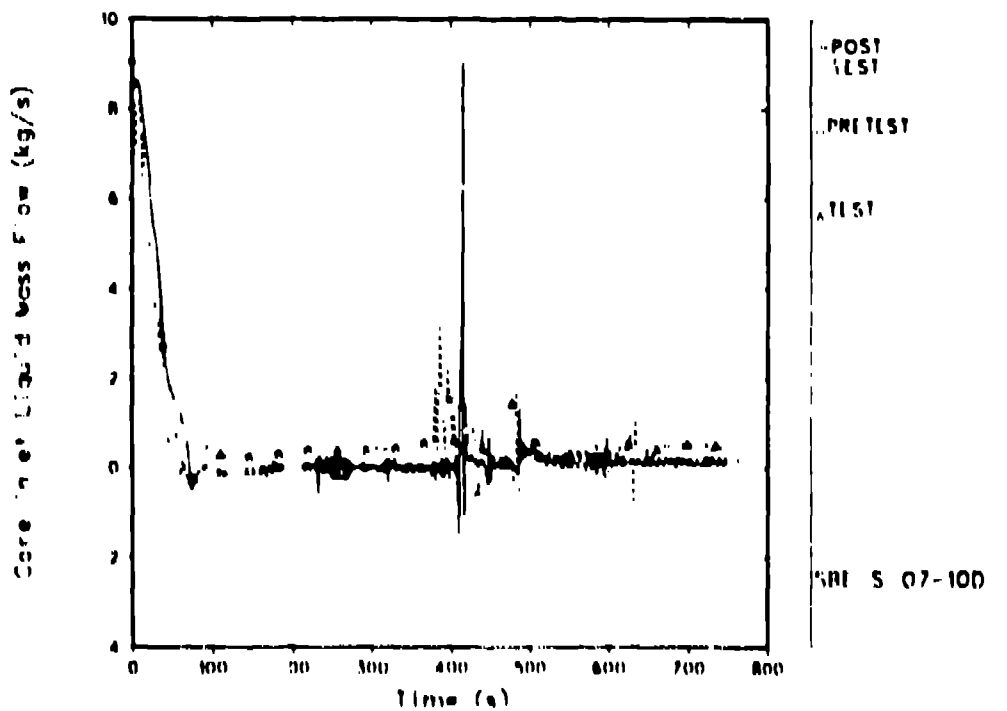


Fig. 16. Core inlet liquid mass flow.

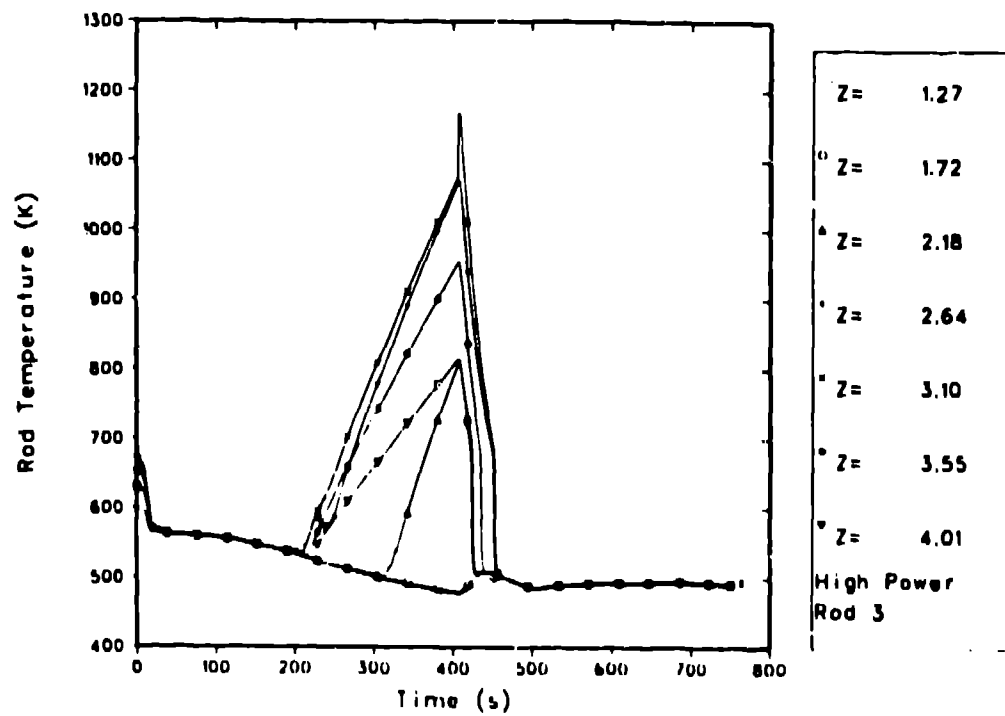


Fig. 17. Rod temperature at various elevations.

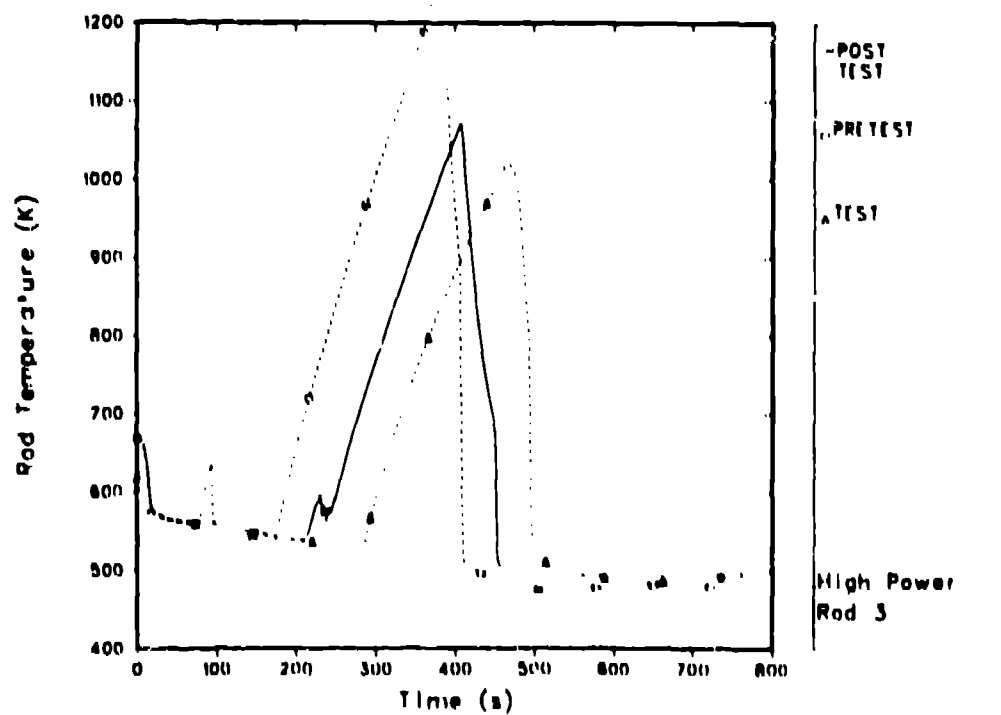


Fig. 18. Comparison of calculated and measured high-power rod temperature.